Evaluation of Component-Aware Dynamic Voltage Scaling for Mobile Devices and Wireless Sensor Networks

Leander B. Hörmann, Philipp M. Glatz, Christian Steger and Reinhold Weiss
Institute for Technical Informatics
Graz University of Technology, Austria
Email: {Leander.Hoermann@, Philipp.Glatz@, Steger@, RWeiss@}TUGraz.at

***Abstract*—Energy efficiency is very important for mobile devices and wireless sensor networks (WSNs), because the consumable energy is limited. Therefore, the operating time of such devices depends mainly on the capacity of the energy storage component and on the average power consumption of the device. The power consumption depends on the supply voltage and on the activated components of the hardware. This work presents the evaluation of component-aware dynamic voltage scaling (CADVS). This low power technique combines the power-down of unused components and the minimization of the supply voltage. Typically, each component of the hardware (microcontroller, transceiver, sensors) has its own supply voltage range. Therefore, the minimum allowed supply voltage depends on the activated components. However, the activated components and consequently the minimum allowed supply voltage varies over time. CADVS uses voltage converter to adjusts the supply voltage of the hardware to save as much energy as possible. This work presents the evaluation of six different voltage converters. It has been shown that CADVS can be used to save up to 38.7 % of the energy compared to a constant voltage supply using the introduced scenario while achieving the same end-user performance.**

***Keywords*-component aware dynamic voltage scaling; dynamic voltage scaling; energy efficient supply; mobile devices; perpetual operation; wireless sensor networks**

I. Introduction and Related Work

Mobile devices and wireless sensor network (WSN) nodes need to be as energy efficient as possible, because their available energy is limited. Mobile devices need their own power source to supply the device everywhere. Typically, they are powered by normal (Alkaline) or rechargeable batteries (nickel-cadmium (NiCd), nickel-metal hydride (NiMH), lithium-ion (LiIon) or lithium-ion polymer (LiPo)). The operating time depends on the power consumption of the device and on the capacity of the batteries. Due to the fact that the devices are portable, the size of the batteries and consequently the available energy is limited.

WSNs are used to measure physical quantities of the environment in application areas with mobility or bad infrastructure. A few examples of application areas are precision agriculture [1], wildlife monitoring [2], human health care [3] and structural health monitoring [4]. Due to the lack of wired infrastructure, each sensor node needs its own energy source. Typically, sensor nodes are powered by batteries or energy harvesting systems (EHSs) [5]–[7]. EHSs use energy harvesting devices to convert environmental energy into electrical energy. The type of the environmental energy source and the efficiency of the energy harvesting device have a high influence on the amount of harvestable energy. Table I shows typical energy harvesting technologies and their power densities [7], [8]. The size of a sensor node is often limited. Consequently, the available power consumption of the WSN node is also limited. Due to the fact, that *energy from the environment is generally unpredictable, discontinuous, and unstable* [10], an energy storage component is needed to bridge periods with insufficient harvestable energy.

Table I
Power densities of different energy harvesting technologies [7], [8].

Harvesting technology	Power density
Solar cells (outdoor at noon)	10-15 mW/cm^2
Solar cells (indoor) [9]	$\approx 10\,\mu W/cm^2$
Piezoelectric (shoe inserts)	$\approx 300\,\mu W/cm^3$
Vibration (small microwave oven)	$\approx 100\,\mu W/cm^3$
Thermoelectric ($10°C$ gradient)	$\approx 40\,\mu W/cm^3$
Acoustic noise (100dB)	$\approx 1\,\mu W/cm^3$

Typical energy storage components are rechargeable batteries and double layer capacitors (DLCs). Table II shows the most common types and their characteristics. It can be seen that the DLC has very low energy density compared to the battery types, but the lifetime of the DLC is much higher. The lifetime is measured in charge-discharge cycles. Here, it indicates the number of charge-discharge cycles which are necessary to reduce the usable capacity of the battery to $80\,\%$ of its nominal value. All the mentioned rechargeable batteries have a lifetime of 500 to 1000 cycles. However, the DLC has a lifetime of up to 500000 cycles.

Table II shows also the start and end voltage of a discharge phase. The terminal voltage of an energy storage component starts at a high voltage (start voltage) and drops down to the end voltage during discharge. If the hardware is designed properly, it is possible to supply the hardware directly. This means the energy storage component is connected to the mobile device or the WSN node directly. Then, the

978-1-4577-0351-5/11/$26.00 ©2011 IEEE

Table II
POSSIBLE BATTERY TYPES AND THEIR CHARACTERISTICS TO SUPPLY MOBILE DEVICES AND WSN NODES [11].

Battery Type	Start Voltage	End Voltage	Average Discharge Voltage	Energy Density
Alkaline	1.5 V	0.7 V	≈ 1.2 V	≈ 145 Wh/kg
NiMH	1.38 V	0.8 V	≈ 1.25 V	≈ 75 Wh/kg
NiCd	1.48 V	0.8 V	≈ 1.26 V	≈ 35 Wh/kg
LiIon	4.1 V	2.5 V	≈ 3.76 V	100 − 158 Wh/kg
LiPo	4.1 V	2.8 V	≈ 3.8 V	136 − 190 Wh/kg
DLC [12]	2.7 V	0.0 V	1.35 V	5 Wh/kg

supply voltage of the hardware is equal to the terminal voltage of the energy storage component. Therefore, the voltage of the fully charged energy storage component must be higher than the minimum allowed supply voltage. The emerging difference is wasted energy which is explained in the following.

The heart of almost all electronic devices is a microprocessor or microcontroller. Typically, it is a digital CMOS (complementary metal oxide semiconductor) circuit. Such a circuit has a static and a dynamic power consumption [13]. The static power consumption results from leakage and bias currents. It can be neglected in systems with a power consumption of more than 1 mW. The dynamic power consumption of a CMOS circuit can be calculated as shown in (1). It is assumed that the switching elements (the gates) of the CMOS circuit have a common switching capacity C.

$$P_{Dynamic} = C \cdot f \cdot V_{Supply}^2 \tag{1}$$

It can be seen that the clock frequency f of the circuit has linear influence and the supply voltage V_{Supply} has quadratic influence on the dynamic power consumption $P_{Dynamic}$. Therefore, much energy can be saved if the supply voltage of devices using CMOS circuits is as low as possible. Voltage conversion circuits are used to convert the terminal voltage of the energy storage components to the desired supply voltage of the hardware. There are different types of such voltage conversion circuits and two of them are explained in Section III.

Another method to save a lot of energy is to switch off the unused hardware components completely. We have described this idea in [14]. The microcontroller of the hardware controls the power supply of the components of a mobile device or a WSN node, e.g. sensors, communication module. They are only switched on if they are needed by the microcontroller.

The combination of the controllable power switches of each component and the minimization of the needed supply voltage results in component-aware dynamic voltage scaling (CADVS). Our previous work [15] describes the theory of this low-power principle in detail.

The rest of the paper is organized as follows: Section II presents the application scenario of a WSN node which is used for further discussion. Section III shows the principles of energy efficient supply of mobile devices and WSN nodes. Therefore, different battery types and different hardware components are considered. Section IV explains CADVS applied to mobile devices and WSN nodes. Section V shows the measurement setup which is used to evaluate the different voltage conversion circuits. Section VI presents and discusses the measurement results of the different circuits with and without CADVS. Finally, Section VII concludes the paper and shows directions for future work.

Table III
HARDWARE COMPONENTS AND THEIR SUPPLY VOLTAGE RANGE.

Hardware Component	Supply Range	$V_{sup,min,component}$
Microcontroller	1.8 V to 3.6 V	1.8 V
Temperature Sensor	3.3 V to 3.3 V	3.3 V
Transceiver	2.4 V to 3.6 V	2.4 V

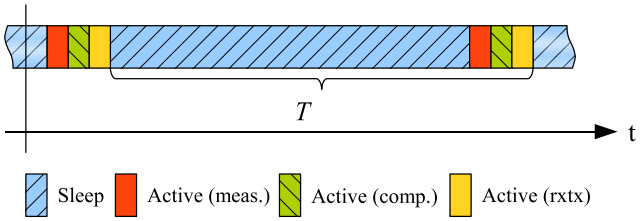

Figure 1. Chronological sequence of an interval T.

II. APPLICATION SCENARIO

This section describes the application scenario and the used hardware components. The goal is to design a low-power WSN node which can be used to measure the temperature of the environment.

The WSN node consists of three main components. The first one is an MSP430F1611 microcontroller from Texas Instruments. It has a supply voltage range from 1.8 V to 3.6 V [16]. The microcontroller is operated at 4 MHz clock frequency to be able to use the full supply range.

The second main component is the precise temperature sensor TMP05B from Analog Devices to measure the temperature of the environment. To achieve an accuracy of 0.2 %, the supply voltage has to be in the range of 3.135 V to 3.465 V [17]. To get the best accuracy, the supply voltage should be 3.3 V.

The third main component is the 2.4 GHz IEEE802.15.4 transceiver module MRF24J40MB from Microchip. Its supply voltage range is from 2.4 V to 3.6 V [18]. Table III lists the main components and their supply voltage ranges.

The chronological sequence of an interval is shown in Figure 1. It is assumed that the sleep state (t_{sleep}) lasts for 85 % of the interval T. The measurement state (t_{meas}), the computation state (t_{comp}) and the communication state (t_{comm}) last for 5 % of the interval T each.

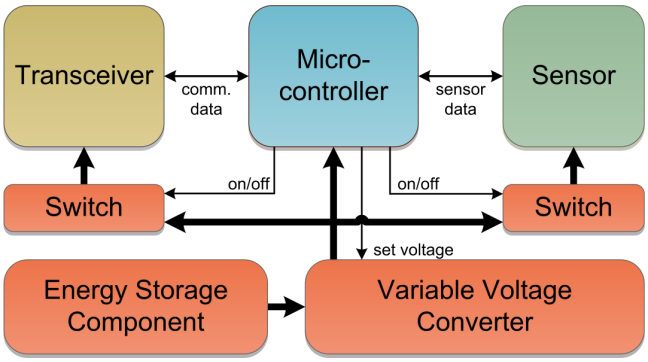

Figure 2. Structure of the WSN node (extended from [19]). The power supply of the sensor and of the transceiver can be switched off by the microcontroller. Furthermore, the variable voltage converter enables CADVS.

III. Energy Efficient Design of Mobile Devices and WSN Nodes

This section describes three low-power principles for an energy efficient design of mobile devices or WSN nodes. It also provides an overview of two common voltage conversion techniques.

The first principle is duty cycling. The microcontroller remains in a power saving sleep state during periods without workload. Therefore, no special hardware is needed, because the MSP430 family supports this feature. This method is often used in low-power mobile devices and WSNs. One interval T is split into an active phase t_{active} and a sleep phase t_{sleep}. The duty cycle can be calculated according to (2).

$$DutyCycle = \frac{t_{active}}{T} \tag{2}$$

The calculation of the duty cycle of the scenario is shown in (3).

$$DutyCycle_{Scenario} = \frac{t_{active}}{T} = \frac{t_{meas} + t_{comp} + t_{comm}}{T} = 15\,\% \tag{3}$$

The second principle is power supply switching. The power supply of the unused components is switched off completely. The hardware must support this feature. The sensor node in Figure 2 uses two power switches controlled by the microcontroller to enable or disable the power supply of the transceiver and the sensor.

The third principle is the minimization of the supply voltage. The supply voltage is set to the minimum allowed value depending on the currently active components. However, the hardware must support this feature. The microcontroller controls the output voltage of variable voltage converter as shown in Figure 2.

Due to the fact that the terminal voltage of the LiIon and the LiPo battery is higher than the maximum allowed supply voltage of the node, a voltage converter is needed to reduce the battery voltage. We discuss only converter circuits which reduce the terminal voltage.

Basically, there are two different types of voltage converters which are explained in the following two sections.

A. Linear Voltage Regulators

Linear voltage regulators provide a constant output voltage by changing its internal resistance depending on the load current. A low-dropout (LDO) regulator is a special type which can operate with a low difference of the input and the output voltage. The voltage drop at the regulator can be calculated using the battery voltage V_{Bat} and the supply voltage of the microcontroller V_{CC} (4).

$$V_{regulator} = V_{Bat} - V_{CC} \tag{4}$$

The average input current of the microcontroller is equal to the average input current of the regulator (5). Quiescent and leakage currents of the regulator are not considered here.

$$I_{regulator} = I_{\mu C} \tag{5}$$

The power consumption can be calculated as shown in (6).

$$P(V_{CC}) = I_{regulator} \cdot V_{Bat} = I_{\mu C}(V_{CC}) \cdot V_{Bat} \tag{6}$$

B. Step Down Converter

Step down converters, also called buck converters, provide a constant output voltage by changing the timing of internal switching elements. Typically, inductors or capacitors are used in combination with these switches. The voltage drop at the converter can be calculated using the battery voltage V_{Bat} and the supply voltage of the microcontroller V_{CC} (7).

$$V_{Buck} = V_{Bat} - V_{CC} \tag{7}$$

However, the average input current of the microcontroller is not equal to the average input current of the regulator (8).

$$I_{Buck,input} \neq I_{Buck,output} = I_{\mu C} \tag{8}$$

The input power is equal to the output power (ideal step down converter). Therefore, the input power depends only on the power consumption of the microcontroller (9).

$$P_{IN}(V_{CC}) = P_{OUT}(VCC) = I_{\mu C}(V_{CC}) \cdot V_{CC} \tag{9}$$

IV. Component Aware Dynamic Voltage Scaling

As mentioned in the introduction, the combination of the controllable power switches of each hardware component and the minimization of the needed supply voltage results in CADVS. The application running on the hardware enables only the needed hardware components. The information of these active components is stored in a list L. The microcontroller is always on the list, because it is supplied all the time in this example.

Each hardware component has its own supply voltage range with a lowest possible supply voltage (LPSV)

Table IV
SUBINTERVALS AND THE NEEDED HARDWARE COMPONENTS.

Phase	Needed Comp. L	Min. allowed volt. list L_{LPSV}	V_{CC}
Sleep	[Microcontroller]	[1.8 V]	1.8 V
Measurement	[Microcontroller, Temp. Sensor]	[1.8 V, 3.3 V]	3.3 V
Computation	[Microcontroller]	[1.8 V]	1.8 V
Communication	[Microcontroller, Transceiver]	[1.8 V, 2.4 V]	2.4 V

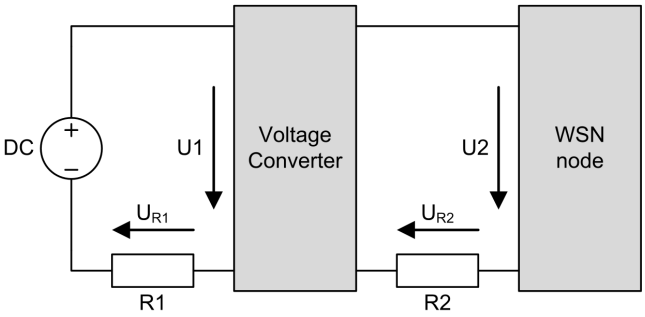

Figure 3. Measurment setup to evaluate CADVS.

$V_{sup,min,component}$. The combination of the list of the active components and the their LPSV results in a list of LPSVs of the active components L_{LPSV}. The optimal supply voltage can be determined as shwon in (10).

$$V_{sup,min,node} = max(L_{LPSV}) \tag{10}$$

The active components change during program execution and therefore, the lists L and L_{LPSV}. Consequently, the optimal supply voltage $V_{sup,min,node}$ changes also during program execution. To save as much energy as possible the supply voltage of the node should be set to this value (11).

$$V_{CC} = V_{sup,min,node} \tag{11}$$

Table IV shows the list of the needed components L of each phase, the list of the minimum allowed supply voltage L_{LPSV} and the resulting supply voltage of the node V_{CC} of the scenario.

V. MEASUREMENT SETUP AND VOLTAGE CONVERTERS

This sections shows the measurement setup and the five different voltage converter circuits which are used to evaluate CADVS. The measurement setup is similar to the setup which we have used to measure EHSs in [20]. It is shown in Figure 3. The NI PXI-6221 DAQ measurement device from National Instruments is used to sample the voltage drop U_{R1} and U_{R2} at the shunt resistors $R1$ and $R2$ as well as the input voltage $U1$ of the voltage converter and the input voltage $U2$ of the WSN node. The value of both shunt resistors is $4\,\Omega$. Therefore, the input power can be calculated as shown in Equation 12.

$$P_{conv,input} = U1 \cdot \frac{U_{R1}}{R1} \qquad P_{node,input} = U2 \cdot \frac{U_{R2}}{R2} \tag{12}$$

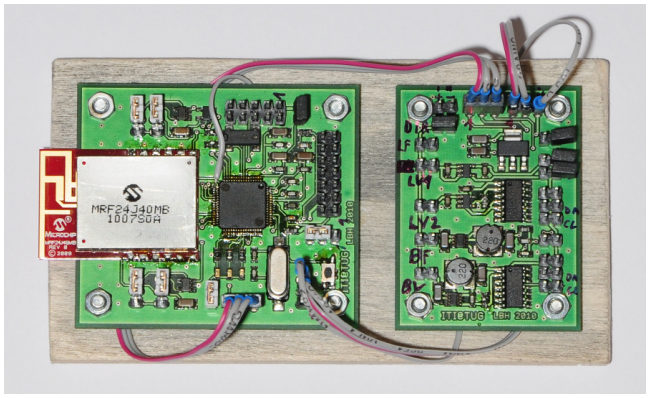

Figure 4. Prototype of the WSN node (left board) and the five different converter circuits (right board).

The sleep current is too low to be measured with this setup. Therefore, a precise multimeter (Fluke 289) with an direct current resolution of $0.01\,\mu$A and an accuracy of $\pm 0.075\,\%+ 0.2\,\mu$A is used. An image of the implemented prototype is provided in Figure 4.

A. Voltage Converter Circuits

The five different voltage converter circuits are shown in Figure 5. The following list describes the different voltage converter circuits.

LDO1FIX: The first circuit (Figure 5(a)) is only implemented to show a bad voltage converter. This converter has a very high quiescent current of 5 mA according to the datasheet [21]. This current is higher than the supply current of the MSP430 at full power mode.

LDO2FIX, LDO2VAR: The second circuit (Figure 5(b)) is used for two measurements. First, it is used to evaluate the LDO regulator circuit with a constant output voltage of 3.3 V (LDO2FIX). Second it is used in a two-step mode (LDO2VAR). This regulator supports the possibility to change the output voltage between two fix values. The selected version of the converter supports 2.2 V and 3.3 V output voltage. Therefore, it can be used for CADVS in a slightly limited way.

BUCK1FIX: The third circuit (Figure 5(c)) shows the implementation of a step down converter with a constant output voltage of 3.3 V.

LDO3VAR: The fourth circuit (Figure 5(d)) is one of the two circuits which enables real CADVS. The output voltage of the LDO regulator can be adjusted by changing the resistance of the digital potentiometer AD5241 between 1.8 V and 3.3 V.

BUCK2VAR: The fifth circuit (Figure 5(e)) is the second circuit which enables real CADVS. The output voltage of the step down converter can be adjusted by changing the resistance of the digital potentiometer AD5241 between 1.8 V and 3.3 V.

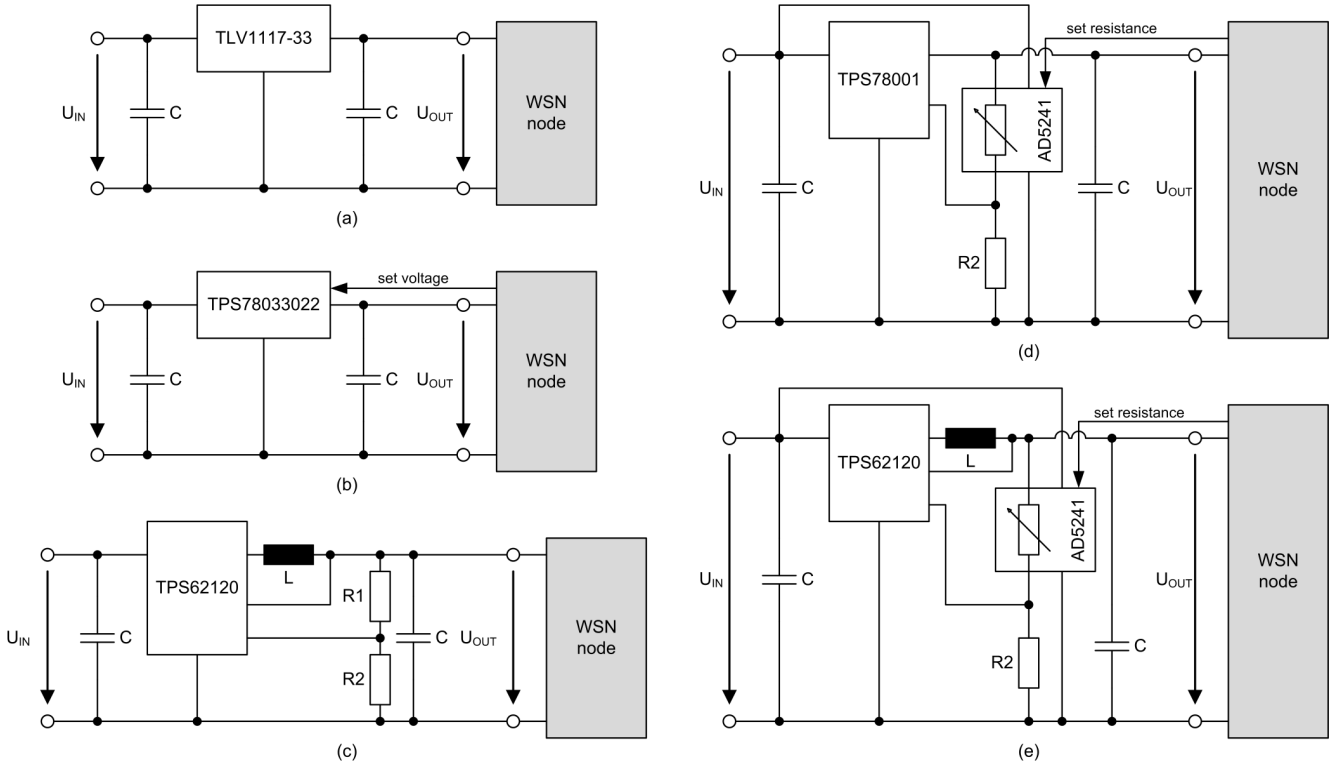

Figure 5. Five different voltage converter circuits which are used to evaluate CADVS. (a) shows the converter circuit using the TLV1117-33 LDO regulator with a constant output voltage of 3.3 V. (b) shows the converter circuit using the TPS78033022 LDO regulator. It is used with a constant output voltage of 3.3 V and with variable output voltage (2.2 V and 3.3 V). (c) shows the converter circuit using the TPS62120 step down converter with a constant output voltage of 3.3 V. (d) shows the converter circuit using the TPS78001 LDO regulator with a variable output voltage (1.8 V to 3.6 V). (e) shows the converter circuit using the TPS62120 step down converter with a variable output voltage (1.8 V to 3.6 V).

VI. Results

This section presents the measurement results of this work. First, the input current and the input power of the WSN node is measured without a voltage converter.

A. Direct Supply

The WSN node is connected to the power supply without using a voltage converter. The supply voltage is varied from 1.8 V to 3.6 V and the input current and power are plotted. This is done for each phase of the interval.

Figure 6 shows the current and power consumption of the WSN node depending on the supply voltage during the sleep phase 6(a), the measurement phase 6(b), the computation phase 6(c) and the communication phase 6(d).

It can be seen that the current consumption has a close-to-dependency on the supply voltage during the measurement and the computation phase. Due to the very low current consumption during the sleep phase, other influences as mentioned in the introduction cause the non- dependency.

B. Converter Output Voltages

The measurement shows the output voltages of the six different converters depending on the input voltage. The results are shown in Figure 7. It can be seen that the LDO1FIX converter has a very high drop voltage. The terminal voltage of the battery must be higher than at the other converters to get an output voltage of 3.3 V. A lot of energy is wasted when using this converter. Therefore, it is unsuitable to supply the WSN node and it is not considered in further results.

The minimum supply voltage at the sleep phase and the computation phase is 1.8 V. Figures 7(a) and 7(c) shows that the LDO3VAR and the BUCK2VAR converter can set this voltage. The LDO2VAR converter cannot set this low voltage. It is only possible to set 2.2 V. The other converters (LDO2FIX and BUCK1FIX) supply the node with a voltage of 3.3 V.

The minimum supply voltage during the measurement phase must be 3.3 V. Therefore, all converter circuits try to set this output voltage.

During the communication phase (Figure 7) the minimum supply voltage is 2.4 V. LDO3VAR and the BUCK2VAR converter can set this voltage. The lower voltage (2.2 V) of the LDO2VAR converter is too low for this phase. Therefore, the output voltage has to be set to 3.3 V to ensure proper functionality. The other converters (LDO2FIX and BUCK1FIX) supply the node with a voltage of 3.3 V.

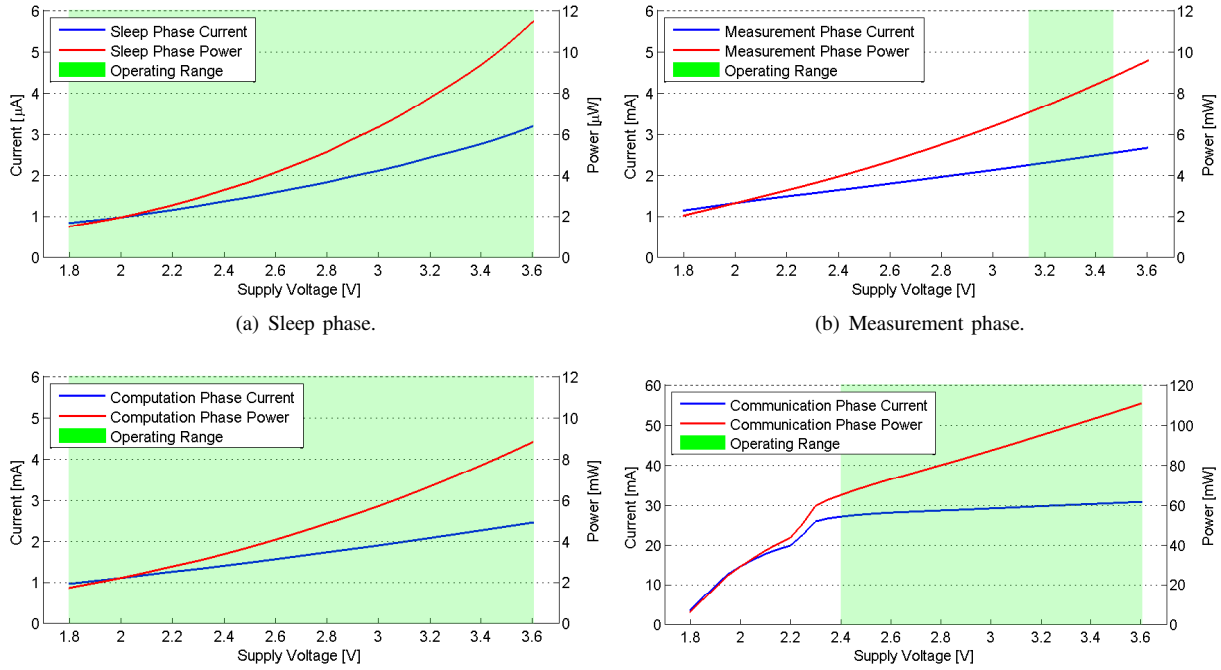

(a) Sleep phase.

(b) Measurement phase.

(c) Computation phase.

(d) Communication phase.

Figure 6. Current and power consumption of the WSN node during the four different phases of the interval depending on the supply voltage of the WSN node.

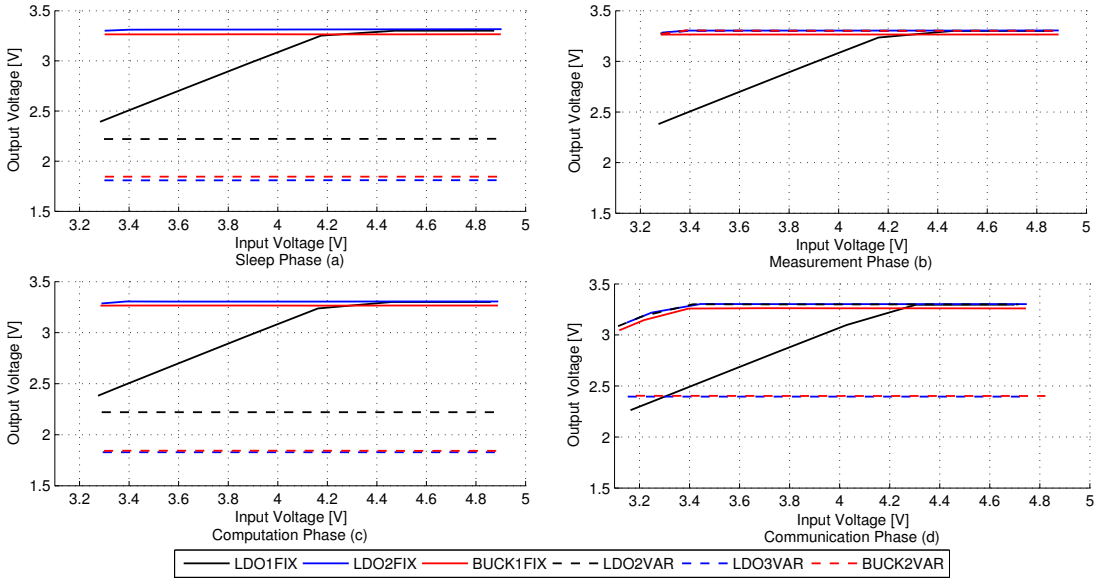

Figure 7. Output voltages of the six different converter circuits depending on the input voltage. (a) shows the output voltages during the sleep phase. (b) shows the output voltages during the measurement phase. (c) shows the output voltages during the computation phase. (d) shows the output voltages during the communication phase.

C. CADVS Results

following. Table V shows the quiescent power of the voltage converter, the overall power consumption (input power of the voltage converter) during the different phases, the efficiency of the voltage converter during the different phases and the power savings compared to the LDO2FIX converter circuit. This converter circuit is used as reference,

Table V
POWER CONSUMPTION, EFFICIENCY AND POWER SAVINGS OF THE FIVE DIFFERENT VOLTAGE CONVERTERS INCLUDING THE QUIESCENT POWER OF THEM. THE AVERAGE VALUES REFER TO THE INTERVAL OF THE SCENARIO. THE INPUT VOLTAGE IS 3.9 V.

Voltage Converter	LDO2FIX	BUCK1FIX	LDO2VAR	LDO3VAR	BUCK2VAR
Quiescent Power of Voltage Conv.	0.5 μW	73.2 μW	0.8 μW	45.7 μW	93.9 μW
Power during Sleep	10.73 μW	83.13 μW	5.38 μW	49.07 μW	97.38 μW
Power during Measurement	9.37 mW	8.25 mW	9.38 mW	9.78 mW	8.90 mW
Power during Computation	8.44 mW	7.42 mW	4.65 mW	3.59 mW	1.63 mW
Power during Communication	95.26 mW	99.45 mW	94.35 mW	81.24 mW	56.89 mW
Average Power	5.71 mW	5.87 mW	5.47 mW	4.83 mW	3.50 mW
Efficiency during Sleep	80.6 %	10.0 %	48.7 %	3.2 %	1.7 %
Efficiency during Measurement	84.9 %	93.2 %	84.6 %	84.3 %	91.9 %
Efficiency during Computation	85.0 %	93.4 %	56.7 %	45.3 %	103.3 %
Efficiency during Communication	87.9 %	94.9 %	88.6 %	63.8 %	91.6 %
Average Efficiency	87.4 %	93.6 %	86.9 %	64.7 %	89.8 %
Power Savings during Sleep	0.0 %	−674.7 %	49.8 %	−357.3 %	−807.5 %
Power Savings during Measurement	0.0 %	12.0 %	−0.1 %	−4.3 %	5.0 %
Power Savings during Computation	0.0 %	12.1 %	44.9 %	57.5 %	80.7 %
Power Savings during Communication	0.0 %	−4.4 %	1.0 %	14.7 %	40.3 %
Average Power Savings	0.0 %	−2.8 %	4.1 %	15.3 %	38.7 %

because it is one of the simplest and cheapest converter circuits.

The results are very interesting. First of all, it can be seen that the quiescent power of the LDO2FIX and the LDO2VAR are much lower than that of the other converters. The high quiescent power of the BUCK1FIX and the BUCK2VAR was expected. The high quiescent power of the LDO3VAR was not expected. It is caused by the supply current of the digital potentiometer and its circuit.

The power consumption during the sleep phase ranges from 5.38 μW to 97.38 μW and this is a big difference. The result is a power saving of −807.5 % during the sleep phase of the BUCK2VAR. The supply power of the WSN node itself ranges from 2 μW at 1.8 V to 8.5 μW at 3.3 V. Therefore, the overall power consumption depends mainly on the quiescent power of the voltage converters BUCK1FIX, LDO3VAR and BUCK2VAR. The two other converters (LDO2FIX and LDO2VAR) have a very low quiescent current. The crucial factor here is the supply voltage of the WSN node. It is 3.3 V at the LDO2FIX converter and 2.2 V at the LDO2VAR converter. This is the reason for the halving of the overall power consumption.

The bad performance of the converter circuits with high quiescent current can also be seen at the efficiency during the sleep phase. During all other phases, the step down converters have the best performance. The regulators cannot achieve such a high efficiency, because they are converting the excess power into heat. However, the 103.3 % is caused by measurement errors. The measurement setup has an error of about 2 % for each power measurement channel as derived in [20].

The power savings of the different voltage converters and the different phases vary very much. As already mentioned, a high quiescent current causes a much higher overall power consumption and consequently a wasting of energy during the sleep phase. During the measurement phase, only the step down converters are able to save power compared to the LDO2FIX converter (reference converter). During the computation phase, the LDO2VAR converter and the LDO3VAR converter perform better than the BUCK1FIX converter, because of the reduced supply voltage of the WSN node. The BUCK2VAR converter performs best, because of the reduced supply voltage and the high conversion efficiency. During the communication phase, only the LDO3VAR converter and the BUCK2VAR converter was able to reduce the supply voltage of the WSN node. Therefore, only these two were able to significantly save power. The bad performance of the BUCK1FIX converter was not expected and can be caused by measurement errors or bad performance of the converter at higher currents. The average power savings during the whole interval clearly show that the BUCK2VAR performs best.

However, the overall power savings heavily depend on the segmentation of the interval. The results are completely different if the sleep phase is much longer than in the scenario. This can be seen in Figure 8. All four plots are based on the measurement results as discussed before. The duration of the sleep phase is varied by keeping the durations of the other phases.

The main result of these four plots is that the lower the duty cycle the better is the LDO2VAR converter. As discussed before, this converter has the lowest quiescent current of the variable voltage converters. The drawback of the only two voltage steps is not important at low duty cycles. The input voltage has no significant influence on the power savings of this converter.

On the other hand the higher the duty cycle is the better performs the BUCK2VAR converter. It has the highest

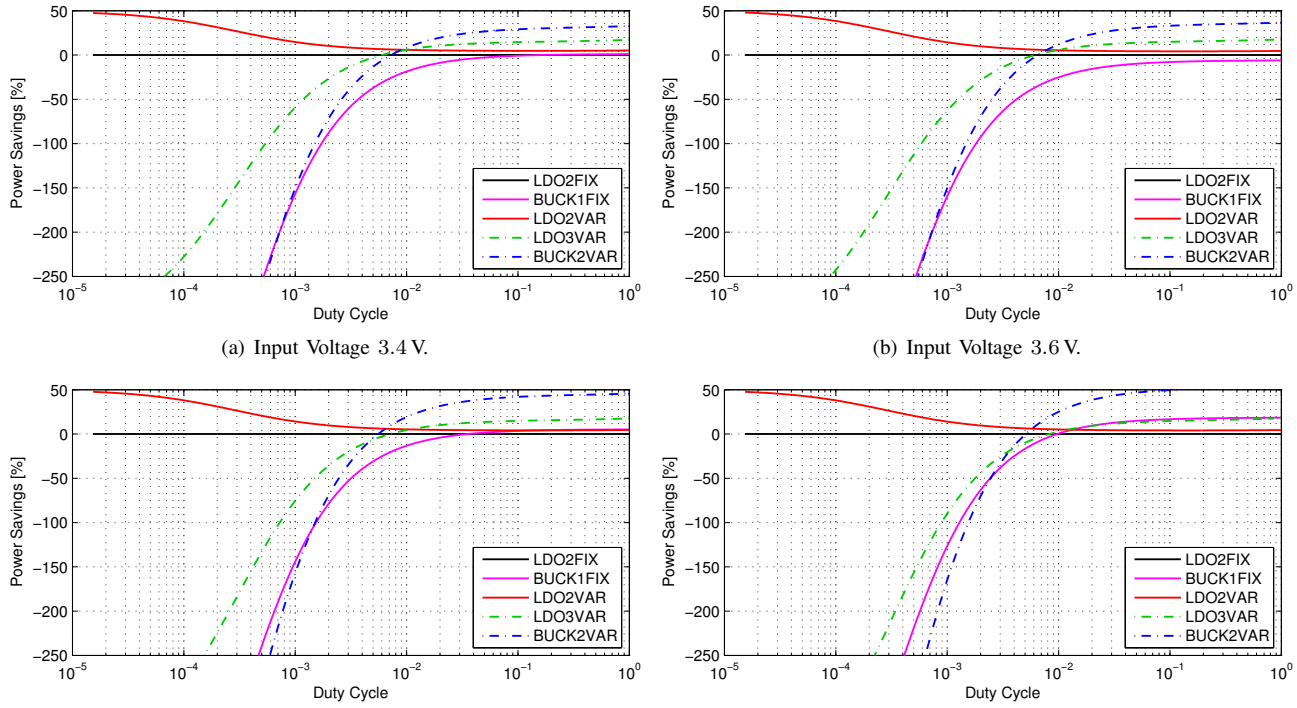

(a) Input Voltage 3.4 V.

(b) Input Voltage 3.6 V.

(c) Input Voltage 4.2 V.

(d) Input Voltage 4.9 V.

Figure 8. Power savings of the five different voltage converter circuits depending on the duty cycle at four differ input voltages of the converters.

efficiency and a variable output voltage. Furthermore, the power savings decrease with decreasing input voltage to over 50 % at 4.9 V.

All these results are also valid for all kinds of mobile devices with low power techniques like duty cycling.

Finally, to achieve best performance on all duty cycles, a combination of the two voltage converters LDO2VAR and BUCK2VAR would perform best. However, the drawback of this solution is the need of extra hardware to switch between these two converters, but it is the best solution for applications with a high variation of the duty cycle. Therefore, the selection of the right voltage converter mainly depends on the specifications of the application running on the mobile device or WSN node.

VII. Conclusion

This work has evaluated different possibilities of the supply of mobile devices or WSN nodes. A realistic scenario has been introduced to get real world results. A prototype has been implemented to evaluate six different voltage converter circuits. It has been shown, that it is possible to save 38.7 % of the energy compared to a constant supply using the introduced scenario while achieving the same end-user performance. In addition, it demonstrated the energy savings depending on the duty cycle of the application. It has been shown, that the leakage currents of the different converter circuits have a high influence at low duty cycles. Therefore, the best converter circuit depends on the application running on the mobile device or WSN node. Future activities will target an improvement of the prototype and a combination of two converters to achieve the best performance over all duty cycles.

References

[1] K. Langendoen, A. Baggio, and O. Visser, "Murphy loves potatoes: experiences from a pilot sensor network deployment in precision agriculture," *Parallel and Distributed Processing Symposium, 2006. IPDPS 2006. 20th International*, p. 8 pp., apr. 2006.

[2] A. Lindgren, C. Mascolo, M. Lonergan, and B. McConnell, "Seal-2-seal: A delay-tolerant protocol for contact logging in wildlife monitoring sensor networks," *Mobile Ad Hoc and Sensor Systems, 2008. MASS 2008. 5th IEEE International Conference on*, pp. 321 –327, sep. 2008.

[3] K. Lorincz, B.-r. Chen, G. W. Challen, A. R. Chowdhury, S. Patel, P. Bonato, and M. Welsh, "Mercury: a wearable sensor network platform for high-fidelity motion analysis," in *SenSys '09: Proceedings of the 7th ACM Conference on Embedded Networked Sensor Systems*. New York, NY, USA: ACM, 2009, pp. 183–196.

[4] N. Xu, S. Rangwala, K. K. Chintalapudi, D. Ganesan, A. Broad, R. Govindan, and D. Estrin, "A wireless sensor network for structural monitoring," in *SenSys '04: Proceedings of the 2nd international conference on Embedded networked sensor systems*. New York, NY, USA: ACM, 2004, pp. 13–24.

[5] R. Min, M. Bhardwaj, S.-H. Cho, N. Ickes, E. Shih, A. Sinha, A. Wang, and A. Chandrakasan, "Energy-centric enabling technologies for wireless sensor networks," *Wireless Communications, IEEE*, vol. 9, no. 4, pp. 28 – 39, aug. 2002.

[6] M. Rahimi, H. Shah, G. Sukhatme, J. Heideman, and D. Estrin, "Studying the feasibility of energy harvesting in a mobile sensor network," *Robotics and Automation, 2003. Proceedings. ICRA '03. IEEE International Conference on*, vol. 1, pp. 19 – 24 vol.1, sep. 2003.

[7] V. Raghunathan, A. Kansal, J. Hsu, J. Friedman, and M. Srivastava, "Design considerations for solar energy harvesting wireless embedded systems," in *Proceedings of the 4th international symposium on Information processing in sensor networks*. IEEE Press, 2005, p. 64.

[8] P. He, Q. Cui, and X. Guo, "Efficient solar power scavenging and utilization in mobile electronics system," *Green Circuits and Systems (ICGCS), 2010 International Conference on*, pp. 641 –645, jun. 2010.

[9] S. Roundy, D. Steingart, L. Frechette, P. Wright, and J. Rabaey, "Power sources for wireless sensor networks," in *Wireless Sensor Networks*, ser. Lecture Notes in Computer Science. Springer Berlin / Heidelberg, 2004, vol. 2920, pp. 1–17.

[10] A. Janek, C. Trummer, C. Steger, R. Weiss, J. Preishuber-Pfluegl, and M. Pistauer, "Simulation based verification of energy storage architectures for higher class tags supported by energy harvesting devices," *Microprocessors and Microsystems*, vol. 32, no. 5-6, pp. 330–339, 2008.

[11] D. Linden and T. B. Reddy, *Handbook of Batteries*, 3rd ed. New York: McGraw-Hill, 2002.

[12] Maxwell Technologies, "Bcap0310 p270 t10 - datasheet - bc power series radial d cell 310f ultracapacitor," http://www.maxwell.com/docs/DATASHEET_DCELL_POWER_1014625.PDF, 2011 February, 1014625.1.

[13] J. Pouwelse, K. Langendoen, and H. Sips, "Dynamic voltage scaling on a low-power microprocessor," in *Proceedings of the 7th annual international conference on Mobile computing and networking*, ser. MobiCom '01. New York, NY, USA: ACM, 2001, pp. 251–259.

[14] L. B. Hörmann, P. M. Glatz, C. Steger, and R. Weiss, "A wireless sensor node for river monitoring using msp430 and energy harvesting," in *European DSP in Education and Research Conference. Proceedings.* Texas Instruments, 2010, pp. 140–144.

[15] ——, "Energy efficient supply of wsn nodes using component-aware dynamic voltage scaling," in *Wireless Conference (EW), 2011 European*, April 2011, pp. 147–154.

[16] Texas Instruments, "Msp430f15x, msp430f16x, msp430f161x mixed signal microcontroller," www.focus-ti.com, SLAS368F, 2009.

[17] Analog Devices, "$\pm 0.5^{\circ}$C accurate pwm temperature sensor in 5-lead sc-70," www.analog.com, D03340 Rev.B, 2006.

[18] Microchip, "Mrf24j40mb data sheet - 2.4 ghz ieee std. 802.15.4 20 dbm rf transceiver module," www.microchip.com, DS70599B, 2009.

[19] D. Puccinelli and M. Haenggi, "Wireless sensor networks: applications and challenges of ubiquitous sensing," *Circuits and Systems Magazine, IEEE*, vol. 5, no. 3, pp. 19–31, 2005.

[20] P. Glatz, L. B. Hörmann, C. Steger, and R. Weiss, "A system for accurate characterization of wireless sensor networks with power states and energy harvesting system efficiency," *Pervasive Computing and Communications Workshops (PERCOM Workshops), 2010 8th IEEE International Conference on*, pp. 468 –473, mar. 2010.

[21] Texas Instruments, "Tlv1117 - adjustable and fixed low-dropout voltage regulator," www.focus-ti.com, SLVS561J, 2004.